Functional and neuropathological changes induced by injection of distinct alpha-synuclein strains: A pilot study in non-human primates

Audrey Fayard, Alexis Fenyi, Sonia Lavisse, Sandra Dovero, Luc Bousset, Tracy Bellande, Sophie Lecourtois, Christophe Jouy, Martine Guillermier, Caroline Jan, et al.

Neurobiology of Disease 180 (2023) 106086

Contents lists available at ScienceDirect

Neurobiology of Disease

journal homepage: www.elsevier.com/locate/ynbdi

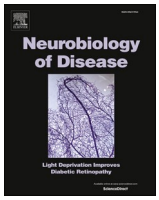

Functional and neuropathological changes induced by injection of distinct alpha-synuclein strains: A pilot study in non-human primates

Audrey Fayard [a,*], Alexis Fenyi [a,1], Sonia Lavisse [a,1], Sandra Dovero [b], Luc Bousset [a], Tracy Bellande [a], Sophie Lecourtois [a], Christophe Jouy [a], Martine Guillermier [a], Caroline Jan [a], Pauline Gipchtein [a], Benjamin Dehay [b], Erwan Bezard [b], Ronald Melki [a], Philippe Hantraye [a,2], Romina Aron Badin [a,2]

[a] CEA, CNRS, Université Paris-Saclay, MIRCen, Laboratoire des Maladies Neurodégénératives, Fontenay-Aux-Roses 92260, France
[b] Univ. de Bordeaux, CNRS, IMN, UMR 5293, Bordeaux F-33000, France

ARTICLE INFO

Keywords:
Non-human primates
Alpha-synuclein strains
Lewy bodies
Nigrostriatal alterations
Alpha-synuclein propagation

ABSTRACT

The role of alpha-synuclein in Parkinson's disease has been heavily investigated since its discovery as a component of Lewy bodies. Recent rodent data demonstrate that alpha-synuclein strain structure is critical for differential propagation and toxicity.

Based on these findings, we have compared, for the first time, in this pilot study, the capacity of two alpha-synuclein strains and patient-derived Lewy body extracts to model synucleinopathies after intra-putaminal injection in the non-human primate brain. Functional alterations triggered by these injections were evaluated *in vivo* using glucose positron emission tomography imaging. Post-mortem immunohistochemical and biochemical analyses were used to detect neuropathological alterations in the dopaminergic system and alpha-synuclein pathology propagation.

In vivo results revealed a decrease in glucose metabolism more pronounced in alpha-synuclein strain-injected animals. Histology showed a decreased number of dopaminergic tyrosine hydroxylase-positive cells in the substantia nigra to different extents according to the inoculum used. Biochemistry revealed that alpha-synuclein-induced aggregation, phosphorylation, and propagation in different brain regions are strain-specific.

Our findings show that distinct alpha-synuclein strains can induce specific patterns of synucleinopathy in the non-human primate, changes in the nigrostriatal pathway, and functional alterations that resemble early-stage Parkinson's disease.

1. Introduction

Synucleinopathies like Parkinson's disease (PD), Dementia with Lew body, or Multiple system atrophy (MSA) are characterized by the aggregation of the pre-synaptic protein alpha-synuclein (α-syn). While under physiological conditions, α-syn is mainly monomeric; it appears aggregated in these various pathological conditions. In PD, these pathological forms of α-syn are constituents of large neuronal inclusions called Lewy bodies (LB) (Spillantini et al., 1997).

Many studies have demonstrated that α-syn aggregates can amplify by recruiting new monomers, spread from cell to cell, and propagate in and outside the brain in a prion-like manner *in vitro* and *in vivo* (Brundin et al., 2010; Jucker and Walker, 2013). This came first with the discovery of α-syn inclusions invading foetal neuronal transplants implanted into the brain of PD patients (Kordower et al., 2008; Li et al., 2008). The injection of viral vectors overexpressing either wild-type or mutant α-syn into the substantia nigra (SN) of rodents and non-human primates (NHPs) led to α-syn pathology propagation and nigrostriatal

Abbreviations: [18F]-FDG, [18F]-fluoro-deoxy-glucose; α-syn, Alpha-synuclein; FIB, Fibrils; GP, Globus Pallidus; LB, Lewy Bodies; moPI, Months Post-injection; MSA, Multiple System Atrophy; NHP, Non-human Primate; PD, Parkinson's Disease; PMCA, Misfolding Cyclic Amplification; RIB, Ribbons; ROI, Region of Interest; SNpc, Substantia Nigra Pars Compacta; TH, Tyrosine Hydroxylase.

* Corresponding author at: DRF/JACOB/MIRCEN/LMNCEA, de Fontenay-aux-Roses, 18 route du panorama, Fontenay-Aux-Roses 92260, France.
E-mail address: Audrey.fayard@cea.fr (A. Fayard).

[1] Second and third authors contributed equally to this work
[2] Last two authors contributed equally to this work

https://doi.org/10.1016/j.nbd.2023.106086
Received 8 February 2023; Received in revised form 13 March 2023; Accepted 15 March 2023
Available online 17 March 2023

changes (Bourdenx et al., 2015; Eslamboli et al., 2007; Kirik et al., 2002; Koprich et al., 2010; Oliveras-Salva et al., 2013). Similarly, the striatal and/or nigral injection of PD-derived LB extracts from parkinsonian patients (Arotcarena et al., 2020; Bourdenx et al., 2020; Recasens et al., 2014), MSA-derived glial cytoplasmic inclusions (GCI) fractions (Teil et al., 2022) or synthetic α-syn fibrils (Chu et al., 2019; Shimozawa et al., 2017; Paumier et al., 2015; Luk et al., 2012) led to variable extents of α-syn pathology and progressive alterations in the dopaminergic system of rodents and NHPs.

α-Syn is a highly dynamic protein. The many conformational states this protein populates allow it theoretically to aggregate into fibrillar assemblies that possess distinct structures and surfaces (as reviewed in Melki 2022) (Melki, 2022). Such structurally distinct fibrillar assemblies, polymorphs or strains seed the aggregation of endogenous α-syn, resist clearance, and bind neuronal cells upon prion-like propagation with different efficiencies (Bousset et al., 2013; Makky et al., 2016; Shrivastava et al., 2020). These properties, together with differential tropism for distinct neuronal cell populations, could explain the heterogeneity within synucleinopathies (Peelaerts et al., 2018; Melki, 2015; Fenyi et al., 2021; Gracia et al., 2020). To confirm this hypothesis *in vivo*, Peelaerts et al. injected different α-syn fibrillar strains called "fibrils" (FIB) and "ribbons" (RIB) into the rat SN or striatum, leading to a strain-specific propagation of α-syn pathology and pathogenic phenotype (Peelaerts et al., 2015).

Here, we build up on the rodent work and scale it up to NHP to validate the existence of a causal link between structure and (dys) function underlying the different synucleinopathies in a species closer, from the evolutionary standpoint to humans. We bilaterally injected FIB ($n = 1$) and RIB (n = 1) α-syn strains in the putamen of NHPs and compared them to patient-derived LB extracts (n = 1) as a proof of concept pilot study. The functional impact of the different α-syn inocula on glucose metabolism was assessed longitudinally *in vivo* for 18 months using [^{18}F]-fluoro-deoxy-glucose ([^{18}F]-FDG) PET imaging. Post-mortem analysis included TH immunocytochemistry to detect nigrostriatal alterations and quantification of phosphorylated α-syn at Ser 129 and aggregated α-syn to assess seeding propensity of the various α-syn inocula. We report here that different α-syn strains can induce distinct functional alterations and changes in the nigrostriatal pathway that resemble early-stage PD in the NHP.

2. Materials and methods

2.1. Preparation of α-synuclein inocula

Human wild-type α-syn was expressed in *E. coli* BL21 DE3 CodonPlus cells and purified as previously described (Ghee et al., 2005). Monomeric, endotoxin free (Pierce LAL Chromogenic Endotoxin Quantification Ki), α-synuclein (250 μM) in 50mMTris–HCl, pH 7.5, 150mMKCl or 5 mM Tris, pH 7.5, was assembled into the fibrillar polymorphs FIB or RIB, respectively, by incubation at 37 °C under continuous shaking in an Eppendorf Thermomixer set at 600 r.p.m. for 7 days (Bousset et al., 2013). The assembly reaction was monitored by thioflavin T binding and the nature of the fibrillar assemblies was assessed by transmission electron microscopy after negative staining with 1% uranyl acetate and limited proteolysis using proteinase K followed by PAGE (Bousset et al., 2013) (Supplementary Fig. 1). The polymorphs Fibrils and Ribbons were centrifuged twice at 15,000*g* for 10 min and re-suspended twice in PBS. Their concentration was adjusted to 500 μM in PBS. They were then fragmented to an average length of 40–50 nm by sonication for 20 min in 2 mL Eppendorf tubes using a Vial Tweeter powered by an ultrasonic processor UIS250 v (250 W, 2.4 kHz; Hielscher Ultrasonic) (Peelaerts et al., 2018) and processed for injection.

The α-*syn*-containing LB extracts purified from the substantia nigra pars compacta (SNpc) of post-mortem brains of parkinsonian patients were generated as previously described (Bourdenx et al., 2020). The samples were obtained from brains collected in a Brain Donation Program of the Brain Bank GIE NeuroCEB run by a consortium of Patients Associations: ARSEP (association for research on multiple sclerosis), CSC (association for research on cerebellar ataxias), France Alzheimer and France Parkinson. The consents were signed by the patients themselves or their next of kin in their name, in accordance with the French Bioethical Laws. The Brain Bank GIE NeuroCEB (Bioresource Research Impact Factor number BB-0033-00011) has been declared at the Ministry of Higher Education and Research and has received approval to distribute samples (agreement AC-2013-1887).

2.2. Animals and surgical injections

Three adult male macaques (*M. fascicularis*, 4.22 ± 0.39 years) were used in this study. Brain tissue from four healthy age-matched monkeys was used for histological analysis. Brain tissue from healthy human controls and parkinsonian patients (French brain bank NeuroCEB) was used for biochemical analysis. Pre- and post-operative MRI scans were performed to determine the coordinates for bilateral intrastriatal injection (post-commissural putamen, −1 mm and -4 mm from anterior commissure) at a constant rate of 3 mL/min. 50 μL of LB were injected into 4 sites (12.88 pg/μl), whereas 6.75 μL of FIB and RIB were injected into 4 sites (5 μg/μl). Injected volumes of the different α-syn inocula were calculated based on previous studies in NHPs (Recasens et al., 2014) and rodents (Peelaerts et al., 2015). Based on previous studies injecting LB in NHPs ending at 14 months post-injection (moPI) reporting only mild alterations (Recasens et al., 2014) or ending at 24moPI and reporting pathology (Bourdenx et al., 2020), and expecting fibrillar strains to have faster kinetics, monkeys were euthanized at 18 moPI. Animals were euthanized by pentobarbital overdose (100 mg/kg, i.v.), transcardially perfused with 0.9% NaCl. Brains were quickly removed after death. The left hemisphere was immediately divided into 4 mm slices and the cingulate cortex, caudate, putamen, globus pallidus (GP), amygdala, and SN punched and flash-frozen for biochemical investigations. The right hemisphere was post-fixed for one week in 10 vol/tissue of 4% paraformaldehyde at 4 °C, and cryoprotected in 20 and then 30% sucrose solution for histochemical analysis.

2.3. PET image acquisition and analysis

[^{18}F]-FDG PET imaging was used to characterize brain metabolism in all inoculated NHPs. Scans were performed at baseline and 6-, 9-, 12- and 18 moPI for each animal on a Concorde Focus220 microPET scanner (Siemens, TN, USA). A 17-min-transmission scan was performed before PET acquisition to allow attenuation correction, followed by 60 min dynamic emission acquisition (160.3 ± 12.0 MBq). PET images were corrected and reconstructed as previously described (Goutal et al., 2020). Integrated PET summed images were created for automatic co-registration with the anatomical MRI using dedicated PMOD® software (PMOD Technologies, 3.6). Cortical and sub-cortical anatomical regions of interest (ROI) (caudate, putamen, GP, amygdala and cingulate, occipital, parietal, temporal and frontal cortices) were automatically delineated on individual MRI images using the CIVM atlas and the Primatologist segmentation pipeline (Balbastre et al., 2017). The Patlak analysis yielded regional Ki estimates and Ki parametric images. The radioactive uptake was quantified by the slope (Ki) using linear fitting between the time-activity curve of the ROI and the cerebellum as a reference region.

2.4. Immunohistochemical staining and stereological quantification

α-Synuclein pathology was assessed by α-syn and phosphorylated α-syn at Ser129 immunochemistry, whereas the integrity of the dopaminergic pathways was evaluated by tyrosine hydroxylase (TH) immunohistochemistry. Floating sections were incubated one night at room temperature with antibodies raised against tyrosine hydroxylase (TH) (Immunostar, 22,941, 1:500), human α-syn (mouse monoclonal clone

syn211, Thermo Scientific, MAS-12272, 1:1000), or human phosphorylated PS129 α-syn (mouse monoclonal clone 11A5, Elan, 1:10000) and then with anti-species peroxidase EnVision system (Dako) and 3,3′-diamino-benzidine. Striatal TH levels (optical density) were compared to a single control NHP. In contrast, α-syn and phosphorylated α-syn levels were compared to those in three healthy controls using ImageJ software. TH stereological counts in the SNpc were compared to those in three healthy controls using a Leica DM6000B motorized microscope coupled with the Mercator software (ExploraNova).

2.5. Biochemical analysis

Punches were then sonicated in 10% (weight: volume) protein misfolding cyclic amplification (PMCA) buffer (150 mM KCl, 50 mM Tris-HCl pH 7.5) by sonication using an SFX 150 Cell Disruptor sonicator. α-Syn was quantified using a filter retardation assay as previously described (Van der Perren et al., 2020). Pathogenic aggregated and phosphorylated α-syn were also quantified using the Cisbio FRET assays (Cisbio, France, cat # 6FASYPEG or 6FSYNPEG, respectively) as described (Van der Perren et al., 2020). Brain homogenates were diluted in PMCA buffer containing monomeric α-syn (100 μM) to a final concentration of 2% (weight:volume), equivalent to 6 mg of tissue. The sample was split into two PCR strips tubes (BIOplastics, Landgraaf, The Netherlands). PMCA amplification was performed as described (Tanudjojo et al., 2021). 5 μL were withdrawn from each tube every hour and diluted in 300 μL of 10 μM of Thioflavin T (ThT). The amplification was monitored by measuring ThT fluorescence using a Cary Eclipse Fluorescence Spectrophotometer (Agilent, Les Ulis, France) with fixed excitation and emission wavelengths at 440 nm and 480 nm, respectively.

All biochemical experiments were duplicated, and data obtained have been compared to healthy human control and patient samples (cingulate cortex, French brain bank NeuroCEB) as a clinical benchmark.

2.6. Statistical analysis

This is a case study, and thus statistical analyses were not performed.

3. Results

3.1. Strain-specific metabolic alterations

We injected two distinct α-syn strains and patient-derived LB extracts into the striatum of NHPs to determine whether their structural and biochemical characteristics lead to different functional alterations in glucose metabolism as an indicator of synaptic activity. Parametric [^{18}F]-FDG PET images were obtained for each timepoint (Fig. 1A), and mean Ki (right and left) was calculated in each ROI (Fig. 1B and Supplementary Fig. 2). Irrespective of the ROI, all NHPs showed a progressive decrease in glucose metabolism up to 9 moPI followed by a progressive recovery for the LB- and FIB-injected animals until 18 moPI or a further progressive decrease for the RIB-injected animal up to 12 moPI that stabilized at 18 moPI. These results suggest that although brain metabolism is globally altered after α-syn injection, the time course, the extent of change, and the regions affected are inoculum-dependent.

3.2. Strain-specific nigrostriatal dopaminergic neurotoxicity

In all NHPs, TH immunoreactivity in the putamen and the caudate nucleus was unaltered compared to the control (Fig. 2A**, left panels and** Fig. 2B). However, morphological changes were observed in the SNpc, such as dendritic or axonal varicosities in TH-positive neurons, indicative of an ongoing neurodegenerative process (Fig. 2A**, right panels**). Stereological counts confirmed a loss of TH-positive cells in the SNpc compared to controls that were most prominent in the LB-injected NHP (−36% for LB, −16% for FIB, and − 22% for RIB) (Fig. 2C).

3.3. Strain-specific patterns of α-synuclein-induced pathology

We assessed endogenous α-syn phosphorylation at Ser129, aggregation, and seeding propensity in several ROI, including cingulate cortex, caudate, putamen, GP, amygdala, and SN.

Overall, immunohistochemistry showed that α-syn levels across all ROIs were similar to those observed in control animals, irrespective of the nature of the inoculum (Fig. 3A and Supplementary Fig. 3A). On the contrary, a marked accumulation of pathogenic S129 phosphorylated α-syn (2log ratio compared to controls) was found in the cingulate cortex and putamen in the LB-injected animal, and, to a lesser extent, in NHP injected with RIB (Fig. 3A and Supplementary Fig. 3B). No LB-like inclusions were found.

Filter trap assay results (Fig. 3B—C) indicate that the amount of aggregated α-syn in all brain regions was either similar or higher (more than 25%) than in parkinsonian patient cingulate cortex. The aggregated and S129 phosphorylated α-syn level was the highest in the RIB-injected animal (especially in the cingulate cortex and the amygdala). Overall, our results show that the patterns of aggregated and S129 phosphorylated α-syn are distinct according to the α-syn inoculum.

We further quantified the seeding propensity of the different inocula in homogenates from the same ROI. We compared the levels of aggregated, and S129 phosphorylated α-syn to those of brain homogenates from parkinsonian patients using Cisbio FRET assays (Fig. 3D and Supplementary Fig. 4A-B). The highest content of aggregated and S129 phosphorylated α-syn were found in the GP in the LB-injected NHP, SN in the FIB-injected NHP, and putamen in the RIB-injected NHP, respectively.

Finally, the seeding efficacy of aggregated and S129 phosphorylated α-syn within the same brain regions was quantified by PMCA and compared to that of patient-derived or human control brain homogenates (Fig. 3E and Supplementary Fig. 5). A strong seeding propensity was observed in the cingulate cortex of the LB-injected NHP and the cingulate cortex, putamen, and GP of the FIB-injected animal, while amplification remained homogeneous across all ROIs in the RIB-injected NHP.

4. Discussion

This pilot study aimed to compare the capacity of two different α-syn strains to model synucleinopathies after intra-putaminal injection in the NHP compared to previously published patient-derived LB extracts (Arotcarena et al., 2020; Bourdenx et al., 2020; Recasens et al., 2014). To our knowledge, we show here, for the first time in the NHP, that structurally and biochemically distinct α-syn strains can induce specific functional, morphological, and biochemical alterations, extending previous observations in rodents (Peelaerts et al., 2015).

Longitudinal *in vivo* [^{18}F]-FDG PET imaging revealed that glucose metabolism was differentially affected depending on the α-syn inoculum. LB and FIB injections induced a transient metabolic decrease up to 9 moPI that reverted to basal level over time. RIB injection progressively reduced synaptic activity, which persisted at 18 moPI. It is noteworthy that two injections of a small volume of aggregated α-syn inocula in the putamen can induce a deactivation not only around the injection site (putamen, caudate nucleus, GP) but also in remote regions such as the thalamus and various cortical areas (cingulate, occipital, parietal, temporal and frontal cortices) as previously reported in other models of striatal dysfunction (Lavisse et al., 2019).

TH stereology in the SNpc evidenced mild and distinct reductions in cell numbers in all three injected-NHPs, associated with clear features of ongoing neurodegeneration like dystrophic neurites and numerous punctate varicosities present along processes. These histological observations were present at the somatic level and not at the terminal level,

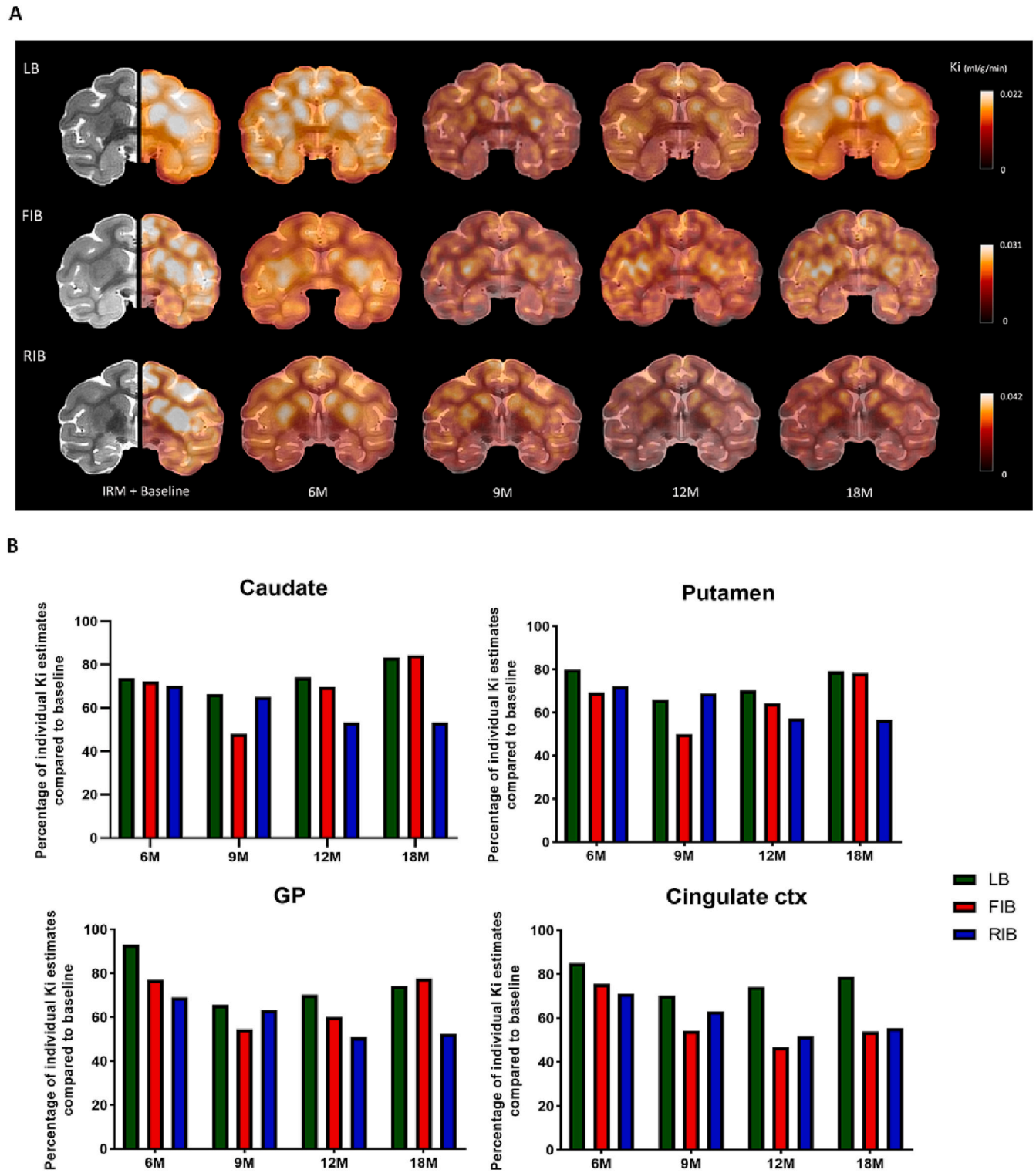

Fig. 1. *In vivo* follow-up analysis by PET [18F]-FDG imaging following LB, FIB, and RIB injection into the striatum of NHPs. (A) Representative coronal PET parametric images at the commissural level were obtained at baseline, 6-, 9-, 12-, and 18-month post-injection (moPI). Parametric images are co-registered to each animal's anatomical MRI image, visible in gray on the left hemisphere in the first column. Ki estimates range from black (no fixation) to white (maximum fixation). (B) Ki values in caudate, putamen, globus pallidus and cingulate cortex at 6-, 9-, 12-, and 18-moPI expressed as a percentage of individual Ki estimates compared to baseline. LB = Lewy body-injected non-human primate, FIB = fibril-injected non-human primate, RIB = ribbon-injected non-human primate, M = months after injection, GP = Globus Pallidus and Ctx = cortex.

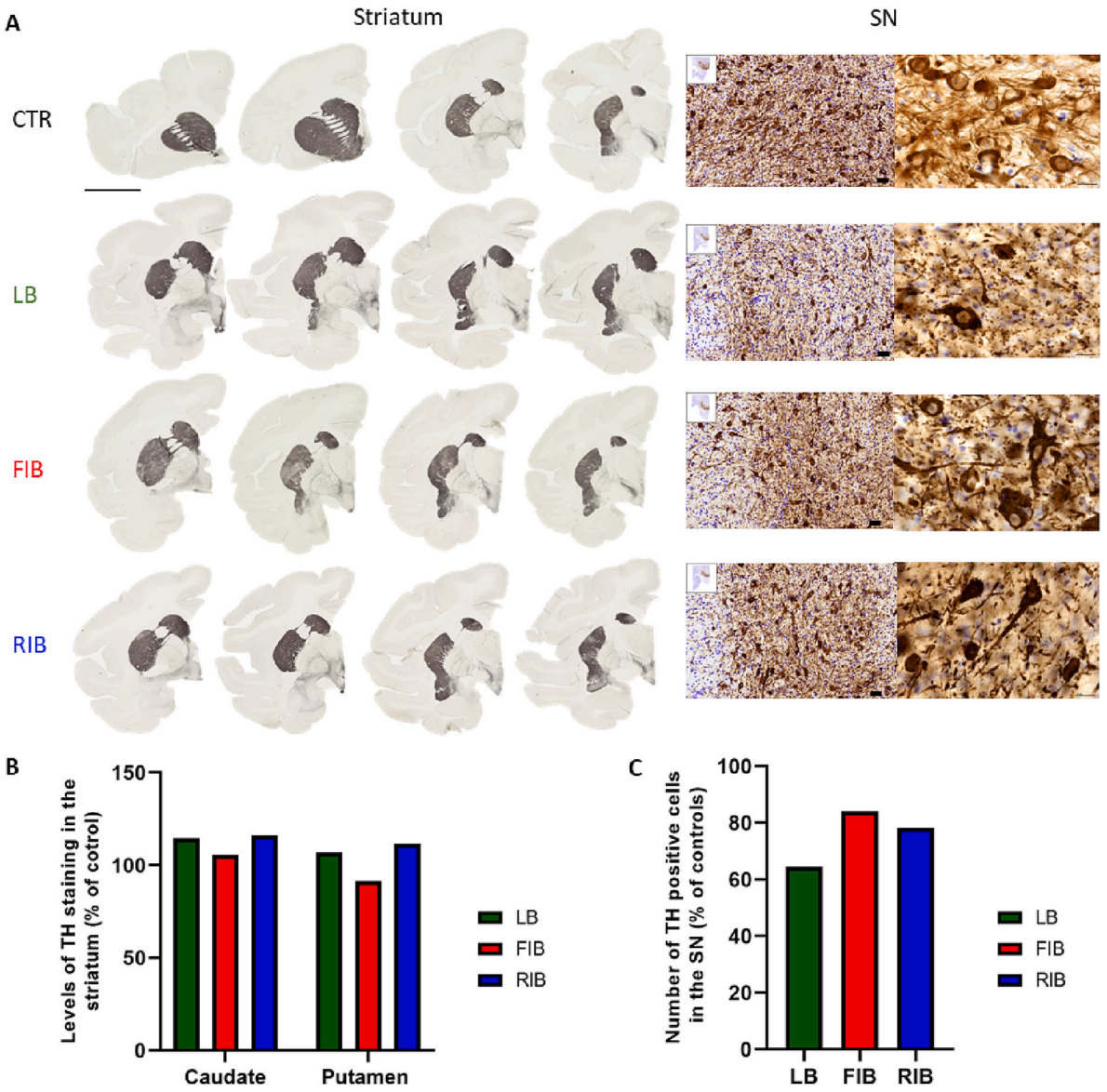

Fig. 2. Changes in TH expression induced by LB, FIB, and RIB injection into the striatum of NHPs at 18 months post-injection. (A) Representative coronal images of TH staining at the striatum (left) and SN (right) levels. (B) Quantification of TH staining by optical densitometry compared to control in caudate nucleus and putamen. (C) Stereological quantification of the number of TH-positive cells in the SN as a percentage of controls. SN = substantia nigra, LB = Lewy body-injected non-human primate, FIB = fibril-injected non-human primate, RIB = ribbon-injected non-human primate. Scale bars = 1 cm (Striatum) and 10 μm (SN).

suggestive of early neurodegeneration that leads to loss of function and precedes axonopathy and cell death, as previously shown (Chu et al., 2019).

Immunohistochemical studies showed that only S129 phosphorylated α-syn was increased in all NHPs across different brain regions close and remote to the injection site. Notably, the increase in S129 phosphorylated α-syn was highest in the LB-injected NHP. Filter trap assays also showed that aggregated α-syn levels were increased in all brain regions in all NHPs, largely exceeding those observed in the patient cingulate cortex. This may be due to the compensatory upregulation of SNCA transcription we recently evidenced after exposing human iPSC-derived dopaminergic neurons to exogenous α-syn strains and seeding endogenous monomeric α-syn aggregation (Tanudjojo et al., 2021). Moreover, this may indicate that the different strains injected, especially the RIB, exhibit higher seeding propensity than the parkinsonian patient case used in our study. This contrasts with the lower phosphorylated α-syn levels observed in all brain regions of all NHPs compared to the patient cingulate cortex. As in the sequence of pathologic events, α-syn aggregation is thought to precede its phosphorylation (Paleologou et al., 2008); our findings suggest that the pathology in our NHPs is at an early phase. Consistent with *in vivo* results, the RIB-injected NHP exhibited the largest α-syn, and S129 phosphorylated α-syn accumulation, not only in the injected region (*i.e.*, putamen) but also remotely, confirming the differential seeding propensity of the strains and suggesting RIBs are more toxic in the NHP brain. The Cisbio FRET assay also revealed that the content of α-syn aggregation is different in the three NHPs, with the highest levels found in the GP (LB), the SN (FIB), and the putamen (RIB), respectively. Together with the PMCA results, this confirms that the seed's structural characteristics dictate their tropism and seeding propensities (Peelaerts et al., 2015).

Although viral overexpression of α-syn with these same strains in rats (Peelaerts et al., 2018) or injection of other synthetic preformed fibrils in NHP[15] have yielded inclusions, the precise link between aggregation and phosphorylation of α-syn *in vivo* needs further substantiation. Some studies suggest that phosphorylation is an early event favoring α-syn aggregation, while others suggest that it is a late event to tag α-syn

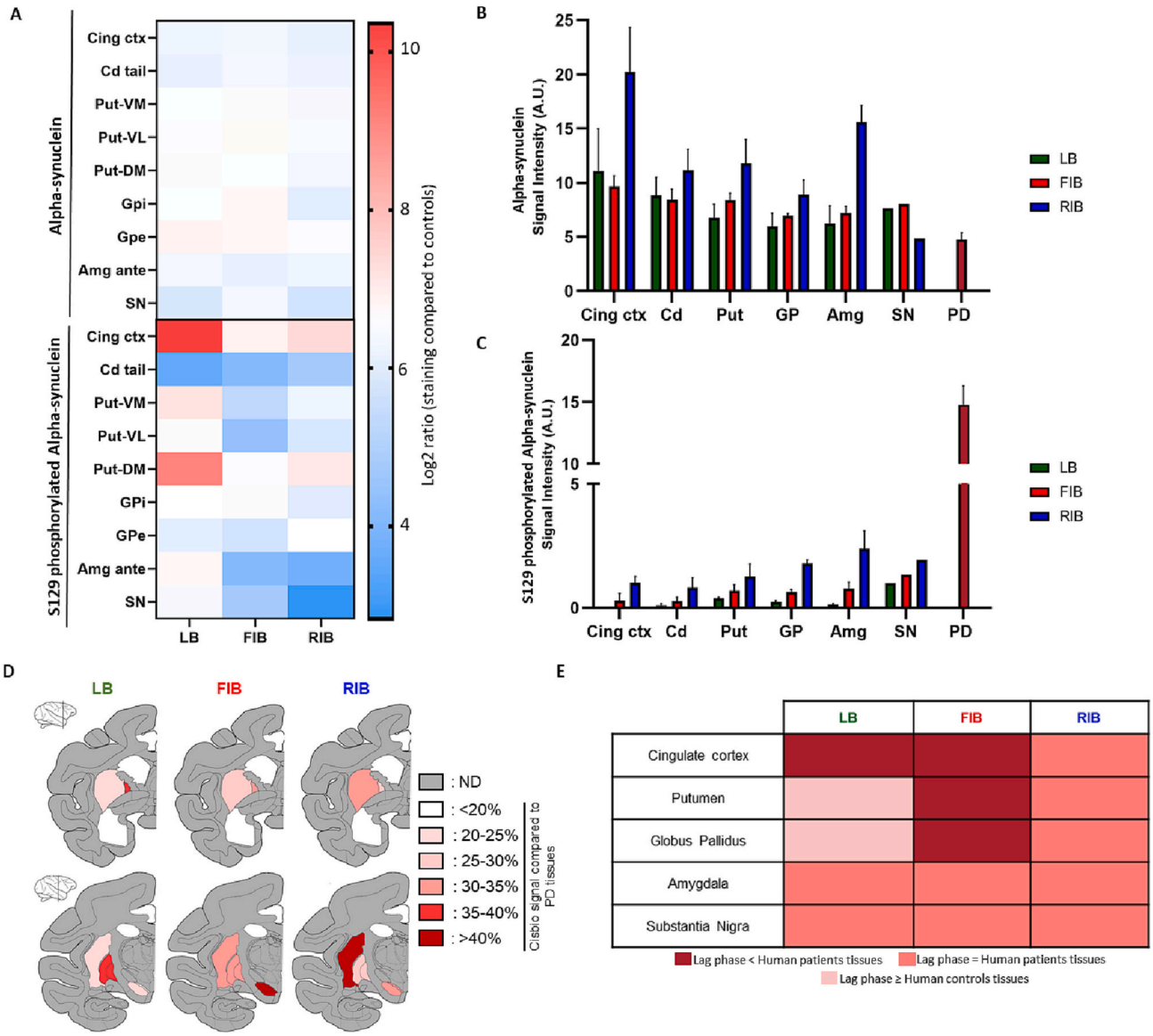

Fig. 3. α-Syn pathology in different brain regions of LB-, FIB-, and RIB-injected NHPs 18 months after injection. (A) Heatmap of the log2 ratios of α-syn and S129 phosphorylated α-syn immunostaining levels in different brain regions compared to controls. (B—C) Filter trap assay quantifications of aggregated and phosphorylated and aggregated α-syn levels throughout different brain regions in NHP compared to Parkinson's disease tissue. (D) Heatmap representing the proportion of aggregated α-syn compared to Parkinson's disease tissue measured by the Cisbio FRET assay. Analyzed brain regions were the cingulate cortex, caudate nucleus, putamen, globus pallidus, amygdala, and substantia nigra. (E) Summary of seeding capacity based on PMCA amplification results in five brain regions. The lag phase in the 2nd round of amplification, assessed by ThT binding, was quantified and compared to samples from Parkinson's disease patients and healthy controls.
All human tissues are from the cingulate cortex. LB = Lewy body-injected non-human primate, FIB = fibril-injected non-human primate, RIB = ribbon-injected non-human primate, Cing ctx = cingulate cortex, Cd = caudate nucleus, Put = putamen, VM = ventromedial, VL = ventrolateral, DM = dorsomedial, Amg = amygdala, Ante = anterior, SN = Substantia nigra.

aggregates for cellular clearance (Oueslati, 2016). Since mature phosphorylated α-*syn*-rich aggregates are typically observed in symptomatic stages of the disease, our finding that aggregated α-syn exhibit low phosphorylation levels suggest that phosphorylation is a late post-translational modification in NHP.

While this proof-of-concept pilot study is encouraging, pending questions await future investigation in a larger number of animals. The LB, FIB, and RIB NHP models generated here exhibit measurable functional alterations that are consistent with an early or prodromal stage of synucleinopathies. The interest of further characterizing and exacerbating these preclinical models in a species close to humans is to identify and test biomarkers and radioligands targeting pathogenic α-syn to better diagnose and stratify patients and evaluate disease-modifying therapeutic strategies at the earliest stages of the disease (Teil et al., 2021).

Funding

This work was supported by the EU Joint Program on Neurodegenerative Disease Research, the Agence National de la Recherche (contracts PROTEST-70, ANR-17-JPND-0005-01, Trans-PathND, ANR-17-JPND-0002-02, SUMMA, ANR-19-17031CE), the Grand Appel d'Offre of the Association France Parkinson (GAO 2019), by the European Union's Horizon 2020 research and innovation program and EFPIA Innovative Medicines Initiative 2 grant agreements No 116060 (IMPRiND), and by the French Investissement d'Avenir Program NeurATRIS (ANR-11-INBS-0011). This study received financial support from the French government in the framework of the University of Bordeaux's IdEx

“Investments for the Future” program/GPR BRAIN_2030.

Credit author statement

Conceptualization: PH, RAB, RM, EB, BD.

Acquisition, analysis, interpretation of data: AF, CJ, PG, SL, MG, SL, RAB, SD, BD, TB, LB.

Have drafted the work or substantively revised it: EB, BD, RM, PH, RAB, SL, AF.

Declaration of Competing Interest

The authors declare no competing interests.

Data availability

The data supporting this study’s findings are available from the corresponding author upon request.

Acknowledgments

The samples were obtained from the Brain Bank GIE NeuroCEB (BRIF number 0033–00011), funded by the patients’ associations France Alzheimer, France Parkinson, ARSEP and ‘Connaître les Syndromes Cérébelleux’ to which we express our gratitude.

Appendix A. Supplementary data

Supplementary data to this article can be found online at https://doi.org/10.1016/j.nbd.2023.106086.

References

Arotcarena, M.L., Dovero, S., Prigent, A., et al., 1 May 2020. Bidirectional gut-to-brain and brain-to-gut propagation of synucleinopathy in non-human primates. Brain. 143 (5), 1462–1475. https://doi.org/10.1093/brain/awaa096.

Balbastre, Y., Rivière, D., Souedet, N., et al., 15 Nov 2017. Primatologist: a modular segmentation pipeline for macaque brain morphometry. NeuroImage. 162, 306–321. https://doi.org/10.1016/j.neuroimage.2017.09.007.

Bourdenx, M., Dovero, S., Engeln, M., et al., 25 Jul 2015. Lack of additive role of ageing in nigrostriatal neurodegeneration triggered by alpha-synuclein overexpression. Acta Neuropathol. Communicat. 3, 46. https://doi.org/10.1186/s40478-015-0222-2.

Bourdenx, M., Nioche, A., Dovero, S., et al., May 2020. Identification of distinct pathological signatures induced by patient-derived α-synuclein structures in nonhuman primates. Sci. Adv. 6 (20) https://doi.org/10.1126/sciadv.aaz9165 eaaz9165.

Bousset, L., Pieri, L., Ruiz-Arlandis, G., et al., 2013. Structural and functional characterization of two alpha-synuclein strains. Nat. Commun. 4, 2575. https://doi.org/10.1038/ncomms3575.

Brundin, P., Melki, R., Kopito, R., Apr 2010. Prion-like transmission of protein aggregates in neurodegenerative diseases. Nat. Rev. Mol. Cell Biol. 11 (4), 301–307. https://doi.org/10.1038/nrm2873.

Chu, Y., Muller, S., Tavares, A., et al., 3 Oct 2019. Intrastriatal alpha-synuclein fibrils in monkeys: spreading, imaging and neuropathological changes. Brain. https://doi.org/10.1093/brain/awz296.

Eslamboli, A., Romero-Ramos, M., Burger, C., et al., Mar 2007. Long-term consequences of human alpha-synuclein overexpression in the primate ventral midbrain. Brain. 130 (Pt 3), 799–815. https://doi.org/10.1093/brain/awl382.

Fenyi, A., Duyckaerts, C., Bousset, L., et al., 12 Jan 2021. Seeding propensity and characteristics of pathogenic αSyn assemblies in formalin-fixed human tissue from the enteric nervous system, olfactory bulb, and brainstem in cases staged for Parkinson’s disease. Cells. 10 (1) https://doi.org/10.3390/cells10010139.

Ghee, M., Melki, R., Michot, N., Mallet, J., Aug 2005. PA700, the regulatory complex of the 26S proteasome, interferes with alpha-synuclein assembly. FEBS J. 272 (16), 4023–4033. https://doi.org/10.1111/j.1742-4658.2005.04776.x.

Goutal, S., Tournier, N., Guillermier, M., et al., 2020. Comparative test-retest variability of outcome parameters derived from brain [18F]FDG PET studies in non-human primates. PLoS One 15 (10), e0240228. https://doi.org/10.1371/journal.pone.0240228.

Gracia, P., Camino, J.D., Volpicelli-Daley, L., Cremades, N., 28 Oct 2020. Multiplicity of α-Synuclein aggregated species and their possible roles in disease. Int. J. Mol. Sci. 21 (21) https://doi.org/10.3390/ijms21218043.

Jucker, M., Walker, L.C., 2013. Self-propagation of pathogenic protein aggregates in neurodegenerative diseases. Review article. Nature. 501, 45. https://doi.org/10.1038/nature12481, 09/04/online.

Kirik, D., Rosenblad, C., Burger, C., et al., 1 Apr 2002. Parkinson-like neurodegeneration induced by targeted overexpression of alpha-synuclein in the nigrostriatal system. J. Neurosci. 22 (7), 2780–2791 doi:20026246.

Koprich, J.B., Johnston, T.H., Reyes, M.G., Sun, X., Brotchie, J.M., 28 Oct 2010. Expression of human A53T alpha-synuclein in the rat substantia nigra using a novel AAV1/2 vector produces a rapidly evolving pathology with protein aggregation, dystrophic neurite architecture and nigrostriatal degeneration with potential to model the pathology of Parkinson’s disease. Mol. Neurodegener. 5, 43. https://doi.org/10.1186/1750-1326-5-43.

Kordower, J.H., Chu, Y., Hauser, R.A., Freeman, T.B., Olanow, C.W., May 2008. Lewy body-like pathology in long-term embryonic nigral transplants in Parkinson’s disease. Nat. Med. 14 (5), 504–506. https://doi.org/10.1038/nm1747.

Lavisse, S., Williams, S., Lecourtois, S., et al., Oct 2019. Longitudinal characterization of cognitive and motor deficits in an excitotoxic lesion model of striatal dysfunction in non-human primates. Neurobiol. Dis. 130, 104484 https://doi.org/10.1016/j.nbd.2019.104484.

Li, J.Y., Englund, E., Holton, J.L., et al., May 2008. Lewy bodies in grafted neurons in subjects with Parkinson’s disease suggest host-to-graft disease propagation. Nat. Med. 14 (5), 501–503. https://doi.org/10.1038/nm1746.

Luk, K.C., Kehm, V., Carroll, J., et al., 16 Nov 2012. Pathological alpha-synuclein transmission initiates Parkinson-like neurodegeneration in nontransgenic mice. Science (New York, N.Y.) vol. 338 (6109), 949–953. https://doi.org/10.1126/science.1227157.

Makky, A., Bousset, L., Polesel-Maris, J., Melki, R., 30 Nov 2016. Nanomechanical properties of distinct fibrillar polymorphs of the protein α-synuclein. Sci. Rep. 6, 37970. https://doi.org/10.1038/srep37970.

Melki, R., 2015. Role of different alpha-Synuclein strains in Synucleinopathies, similarities with other neurodegenerative diseases. J. Parkinsons Dis. 5 (2), 217–227. https://doi.org/10.3233/jpd-150543.

Melki, R., 3 Jun 2022. Disease mechanisms of multiple system atrophy: what a parallel between the form of pasta and the alpha-synuclein assemblies involved in MSA and PD tells us. Cerebellum (London, England). https://doi.org/10.1007/s12311-022-01417-0.

Oliveras-Salva, M., Van der Perren, A., Casadei, N., et al., 25 Nov 2013. rAAV2/7 vector-mediated overexpression of alpha-synuclein in mouse substantia nigra induces protein aggregation and progressive dose-dependent neurodegeneration. Mol. Neurodegener. 8, 44. https://doi.org/10.1186/1750-1326-8-44.

Oueslati, A., 2016. Implication of alpha-Synuclein phosphorylation at S129 in Synucleinopathies: what have we learned in the last decade? J. Parkinsons Dis. 6 (1), 39–51. https://doi.org/10.3233/jpd-160779.

Paleologou, K.E., Schmid, A.W., Rospigliosi, C.C., et al., Jun 13 2008. Phosphorylation at Ser-129 but not the phosphomimics S129E/D inhibits the fibrillation of alpha-synuclein. J. Biol. Chem. 283 (24), 16895–16905. https://doi.org/10.1074/jbc.M800747200.

Paumier, K.L., Luk, K.C., Manfredsson, F.P., et al., Oct 2015. Intrastriatal injection of pre-formed mouse α-synuclein fibrils into rats triggers α-synuclein pathology and bilateral nigrostriatal degeneration. Neurobiol. Dis. 82, 185–199. https://doi.org/10.1016/j.nbd.2015.06.003.

Peelaerts, W., Bousset, L., Van der Perren, A., et al., 18 Jun 2015. Alpha-Synuclein strains cause distinct synucleinopathies after local and systemic administration. Nature 522 (7556), 340–344. https://doi.org/10.1038/nature14547.

Peelaerts, W., Bousset, L., Baekelandt, V., Melki, R., Jul 2018. α-Synuclein strains and seeding in Parkinson’s disease, incidental Lewy body disease, dementia with Lewy bodies and multiple system atrophy: similarities and differences. Cell Tissue Res. 373 (1), 195–212. https://doi.org/10.1007/s00441-018-2839-5.

Recasens, A., Dehay, B., Bove, J., et al., Mar 2014. Lewy body extracts from Parkinson disease brains trigger alpha-synuclein pathology and neurodegeneration in mice and monkeys. Ann. Neurol. 75 (3), 351–362. https://doi.org/10.1002/ana.24066.

Shimozawa, A., Ono, M., Takahara, D., et al., 2 Feb 2017. Propagation of pathological α-synuclein in marmoset brain. Acta Neuropathol. Communicat. 5 (1), 12. https://doi.org/10.1186/s40478-017-0413-0.

Shrivastava, A.N., Bousset, L., Renner, M., et al., 24 Mar 2020. Differential membrane binding and seeding of distinct α-synuclein fibrillar polymorphs. Biophys. J. 118 (6), 1301–1320. https://doi.org/10.1016/j.bpj.2020.01.022.

Spillantini, M.G., Schmidt, M.L., Lee, V.M., Trojanowski, J.Q., Jakes, R., Goedert, M., 28 Aug 1997. Alpha-synuclein in Lewy bodies. Nature. 388 (6645), 839–840. https://doi.org/10.1038/42166.

Tanudjojo, B., Shaikh, S.S., Fenyi, A., et al., Jun 21 2021. Phenotypic manifestation of α-synuclein strains derived from Parkinson’s disease and multiple system atrophy in human dopaminergic neurons. Nat. Commun. 12 (1), 3817. https://doi.org/10.1038/s41467-021-23682-z.

Teil, M., Arotcarena, M.L., Dehay, B., Mar 9 2021. A new rise of non-human primate models of synucleinopathies. Biomedicines 9 (3). https://doi.org/10.3390/biomedicines9030272.

Teil, M., Dovero, S., Bourdenx, M., et al., 29 Apr 2022. Brain injections of glial cytoplasmic inclusions induce a multiple system atrophy-like pathology. Brain 145 (3), 1001–1017. https://doi.org/10.1093/brain/awab374.

Van der Perren, A., Gelders, G., Fenyi, A., et al., Jun 2020. The structural differences between patient-derived α-synuclein strains dictate characteristics of Parkinson’s disease, multiple system atrophy and dementia with Lewy bodies. Acta Neuropathol. 139 (6), 977–1000. https://doi.org/10.1007/s00401-020-02157-3.